Effects of Temperature and Centrifugal Force on Fretting Wear of Contact Interface of Face Gear

AN Xiuli[1], *PEI Dahai*[1], *XIE Kun*[2]

1. Xi'an Shaangu Power Co., Ltd, Xi'an 710075, P. R. China;
2. School of Aerospace Engineering, Xi'an Jiaotong University, Xi'an 710049, P. R. China

(Received 24 June 2020; revised 14 September 2020; accepted 25 September 2020)

Abstract: Taking the typical face gear connection structure of the combined rotor as the research object, this paper studies the distribution rules of the contact state, contact stress and slip distance of the contact tooth surface of face gear under different centrifugal force and temperature conditions by using the finite element method, in order to improve the reliability of face gear connection structure. And the influence of centrifugal force and temperature on the maximum wear depth of the tooth surface is studied based on the fretting wear model proposed by McColl. Results show that: (1) The external diameter has an opening phenomenon on the contact surface of the face gear under the centrifugal effect, which reduces the load-bearing area; (2) The contact stress at the inner root of the face gear is the largest and the wear is the most serious; (3) The temperature field causes the contact surface to be thermally expanded, resulting in the large uneven deformation, and the tooth surface appears drum-shape; (4) The maximum contact stress and the maximum wear depth occur in the middle of the tooth root; (5) As the temperature increases, the maximum wear depth of the tooth surface increases significantly. Consequently, reducing temperature of the combined rotor plays an important role in effectively reducing the wear of the face gear and improving the connection life of face gear connection structure.

Key words: face gear; fretting wear; contact stress; wear depth; fretting wear model

CLC number: V232.9 **Document code:** A **Article ID:** 1005-1120(2020)05-0768-10

0 Introduction

The connecting structures of face gear have many desirable features, including strong load bearing capacity, high stiffness, good stability, reliable positioning, and automatic centering. Therefore, they are widely used in the connections between rotors and discs and the ones between discs of aircraft engines and combined gas turbines. For example, face gear structures are successfully used to achieve connection and transfer the torque between the compressor discs of the center tie rod combined rotors in CT7 turboshaft engines and the turbine discs of the peripheral tie rod combined rotors in Mitsubishi F-class heavy gas turbines[1-2]. In terms of the connecting structure of face gear, fretting wear is the most common form of damage under the complex load of centrifugal force and high temperature in an extended period of service, which leads to the tooth surface wearing, the biting surface loosening and the propagation of cracks on the tooth surface[3-4]. Such damage will greatly shorten the service life of the connecting structure between face gears.

To improve the quality of connections, researchers have extensively studied the stress on the connecting structures of face gear. Pisani et al.[5] used the finite element method and the boundary element method for calculating the two-dimensional and three-dimensional characteristics of stress and obtained the stress distribution on a tooth surface.

*Corresponding author, E-mail address: 18612791374@163.com.

How to cite this article: AN Xiuli, PEI Dahai, XIE Kun. Effects of temperature and centrifugal force on fretting wear of contact interface of face gear[J]. Transactions of Nanjing University of Aeronautics and Astronautics, 2020, 37(5): 768-777.

http://dx.doi.org/10.16356/j.1005-1120.2020.05.011

Richardson et al.[6] are the first ones to compare finite analysis results with experimental test results, and concluded that the finite element calculation results were reliable as long as the quality of the connecting structure was sound. Their results served as the basis for subsequent finite element analyses of the stress characteristics of face gear. Yuan et al.[7] considered the nonlinear contact and calculated the stress distribution on a tooth surface under pre-tensioning, pre-heating, starting, and operating conditions with the finite element method. Yuan et al.[8] investigated the dynamic effect of one detuned tie rod on a rotor, folded the obtained dynamic response curve of the rotor into the finite element model of face gear, and analyzed the effects on the circumferential stress distribution of a single detuned tie rod. Their analysis results showed that the differential of the circumferential stress distribution of face gear was reduced when the negatively detuned tie rod was on the compressed side of a dynamically curved rotor. When the detuned tie rod was on the stretched side, the differential of the circumferential stress distribution was increased. Li et al.[9] performed theoretical analysis and finite element simulation of the tooth surface stress of disc face gear during pre-tensioning and torque-transfer states and validated their theoretical model. Lu[10] studied the variation behavior of tooth surface stress during pre-tensioning, acceleration and torque-transferring stages, and simultaneously analyzed the effects of the geometrical structure on the maximum contact stress of the tooth surface. Shen et al.[11] analyzed the force characteristics of the connecting structure of face gear in a turboshaft engine and pointed out the important role played by the rotational speed and the pre-tensioning force on the contact condition of the tooth connection. And they performed a further finite element study of the effect of rotational speed and pre-tensioning force on the contact condition and the maximum contact stress of tooth surface. Choi et al.[12] also conducted stress and strength estimations for a face gear structure. Li[13] predicted the fatigue life of an arc tooth by the fretting fatigue test for a simulated component of aircraft engines that took into account the effects of the fretting fatigue. However, the current research on face gear contact is mostly limited to the analysis of the force and rarely touches upon the state of wear of the contact surface, except Jiang et al.[14] used the Archard wear formula and the contact mechanics theory to investigate the variation behavior of contact stress, contact width, gap size, and slide distance of the wedge contact surfaces of gas turbine face gear under different alternating loads.

In this study, the connection structure of typical face gear in a combined rotor is examined, and the contact state and the distribution behavior of contact stress and slide distance are discussed under different centrifugal force and temperature conditions. The effects of centrifugal force and temperature loading on the maximum contact stress and the maximum wear depth on the tooth surface are also presented. The conclusions can serve as reference for the design and engineering application of the face gear connection structure.

1 Finite Element Model of Face Gear Connection

1.1 Geometric parameters of face gear

Table 1 shows the calculated and analyzed geometric parameters of the face gear in this paper. The two meshed discs have the same trapezoidal teeth. The inner diameter of the disc is 780 mm and the outer diameter is 820 mm. The positions on the tooth surface are marked according to the meshing situation: The root position is designated as a_1, the center position as a_2, and the tip position as a_3, which all are within the tooth surface meshing range, as shown in Fig.1.

Table 1 Geometric parameters of face gear connection

Parameter	Value	Parameter	Value
Number of teeth	120	Tip height / mm	2.600
Stress angle / (°)	30	Root height / mm	3.266
Outer diameter / mm	820	Tip clearance / mm	0.666
Inner diameter / mm	780	Friction factor μ	0.33
Total height / mm	5.866	Mass density / (kg•m^{-3})	7 850

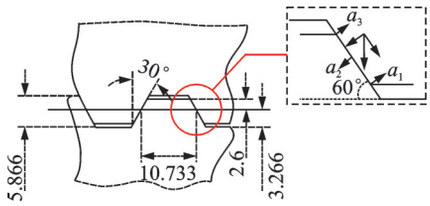

Fig.1 Geometric parameters of face gear

1.2 Finite element model of a face gear

Based on the parameters listed in Table 1, a three-dimensional finite element model for a face gear connection structure is established, as shown in Fig.2. Two disc components are connected with pre-tension using 12 uniformly distributed circumferential tie rods. As shown in Fig.2(a), the component B only retains the axial rotational degree of freedom, while the other degrees of freedom are fixed. A torque load is applied through the reference point on the exterior surface of the component A. It is necessary to ensure that the surface of the torque coupling does not include the contact surface of the face gear so that the contact surface analysis is not affected by the torque application method[15]. The pretension of the tie rod is applied in the form of a bolt load at each tie rod hole. As shown in Fig.2(b), the direction of the tooth length is from the inner diameter to the outer diameter of the tooth, and the length is 20 mm. The direction of the tooth height is from the root to the tip of the tooth along the contact line. Since the relative movement of the contact surface of the discs is a fretting slide, the heat generated by the fretting friction at the contact surface of the discs can be neglected under the normal operating conditions of the rotor, compared with the heat generated by the external heat flow of the disc rim. To simplify the calculation, it is assumed that the stress field generated by the fretting friction will not affect the temperature field. Therefore, a sequential thermo-mechanical coupling[16] simulation calculation is adopted in this study. That is, the temperature field distribution and the thermal stress and strain fields caused by the expansion due to the temperature rise are calculated in the first load step. After that, while keeping the temperature field analysis results unchanged with the boundary condition, pre-tension, torque and centrifugal force are applied to the disc, and the contact attributes of the disc face gear with the temperature field are calculated. Since the stop-run-stop (0-max-0) process of the engine is simulated in this study and the main concern is the influence of speed on the centrifugal load, we adopt the speed loading spectrum shown in Fig.3. When the engine stops, the speed decreases to zero, which is the valley of the load spectrum, and the corresponding stress-strain slide distance decreases to zero. The maximum running speed is the peak of the entire load spectrum. For different peak speeds, the frequency used in the calculation of the load spectrum is the same. With this premise and for the convenience of calculation, we assume that the relative slide distance, the stress and strain changes in a half cycle (0-max) of the periodic load are all unchanged. Therefore, the relative slide distance in the total number of cycles can be obtained by calculating the relative slide distance in one half-cycle. Because of this, next we will focus on the stress-strain and relative slide distance in a half-cycle (0-max).

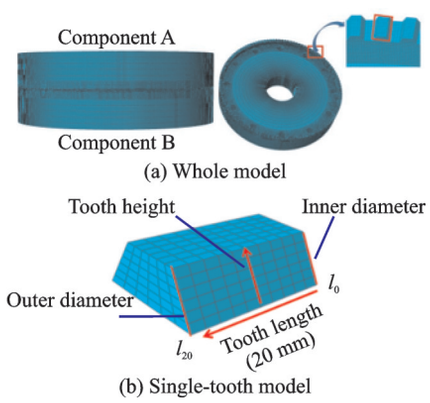

Fig.2 Finite element model of face gear

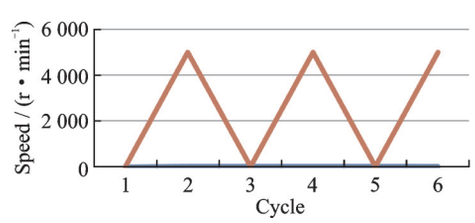

Fig.3 Schematic diagram of rotational speed load spectrum

Ref.[17] showed that the temperature of the combined rotor turbine disc was not uniform in the axial direction under rated conditions, but the maxi-

mum temperature did not exceed 500 ℃. Following a previous report[18], we use the thermos-physical properties of the face gear disc material listed in Table 2 in the calculation.

Table 2 Thermal physical performance parameters of face gear

Temperature /℃	Elastic modulus E / GPa	Poisson's ratio υ	Coefficient of linear expansion $\alpha/(10^6\ ℃^{-1})$
20	209	0.269	—
200	202	0.290	12.4
300	196	0.312	13.1
400	186	0.309	13.6
500	174	0.305	14.4

1.3 Fretting wear model

The study of McColl et al.[19] suggested that fretting wear might be solved by applying the sliding wear Archard formula to each fret width of a contact region. The Archard equation[20] is shown as

$$\frac{V}{S}=K\frac{P}{H} \tag{1}$$

where V is the wear volume, S the relative slide distance, K the wear coefficient, P the normal load, and H the hardness of the material.

Based on the Archard equation, McColl et al.[19] derived and established a fretting wear model in the following form

$$\frac{\mathrm{d}h(x)}{\mathrm{d}s(x)}=k_l p(x) \tag{2}$$

where k_l is the fretting wear coefficient, with a value to be determined by the K/H factor in the Archard equation. This coefficient can also be obtained from the fretting wear test, $p(x)$ is the contact stress at node x, and $s(x)$ the slide distance at node x. From Eq.(2), it can be recognized that $k_l p(x)\mathrm{d}s(x)$ represents the energy dissipation during fretting wear. That is, the fretting wear model proposed by McColl assumes that the fretting depth depends on the contact surface energy dissipation.

We adopt the fretting wear model (Eq.(2)) proposed by McColl in this paper. Because it was in a differential form, Eq.(2) needs to be integrated over half a cycle during the numerical calculation process, namely

$$\int_{N=0}^{N=1}\mathrm{d}h(x,t)=\int_{N=0}^{N=1}k_l p(x,t)\mathrm{d}s(x,t) \tag{3}$$

where $p(x,t)$, $s(x,t)$ and $h(x,t)$ are the contact stress, slide distance and fret wear depth at node x during an incremental time step t, respectively. Since the load simulated in this study is a linear load, we assume for the convenience of integration that there is a linear relationship between $p(x,t)$ and $s(x,t)$. Finally, Eq.(3) is integrated over half a cycle and the result is shown as

$$\Delta h=k_l(p_{\max}-p_{\min})(s_{\max}-s_{\min}) \tag{4}$$

where Δh is the wear depth within half a cycle, $p_{\max}$ and $p_{\min}$ are the maximum and minimum contact stresses within the half cycle, respectively, and $s_{\max}$ and $s_{\min}$ are the maximum and minimum relative slide distances of the half cycle, respectively. As stated in Section 1.2, the load cycle chosen in this study is periodic, so the total wear depth is simply twice Δh multiplied by the total number of cycles. For ease of discussion, we only use the results for half a cycle.

1.4 Relative slide distance of tooth surface

In terms of the contact surface of face gear, the relative slide distance required in the calculation of the fretting wear depth at a node can be divided into slide distance in two directions, as shown in Fig.4, where δ_1 and δ_2 are the axial component (tooth length direction component) and the radial component (tooth height direction component) of the relative slide distance of each node of the tooth surface, respectively. And the total relative slide distance for a node is given by

$$\delta_s=\sqrt{\delta_1^2+\delta_2^2} \tag{5}$$

For all nodes on the contact surface, the total relative slide distance can be obtained by Eq.(5), and then the slide distance distribution on the entire

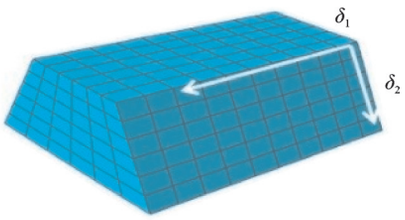

Fig.4 Components of slide distance at a node

contact surface can be obtained.

2 Calculation Results and Analysis

2.1 Effects of rotational speed on fretting characteristics of face gear connection

The tangential force produced by the centrifugal force is proportional to the square of the rotational speed. At a higher rotational speed of the rotor, a greater tangential force is produced, which has a greater impact on the contact condition of the tooth surface. At a torque of $T = 2\ 400$ N·m and a pre-tension of $P = 7.5$ kN, the distributions of the contact stress and the elastic deformation on the tooth surface at different rotational speeds are shown in Figs.5 and 6, respectively. Fig.5 shows that the centrifugal force increases with the increasing rotational speed and it has an increasing effect on the contact conditions of the face gear. Since the pre-tension of the tie rod acted on the inner diameter side of the tooth, the effect of the centrifugal force is to gradually separate and open up the outer diameter side. The greater the centrifugal force is, the more the outer portion of the contact surface opens up. So the load-bearing region becomes smaller and more concentrated towards the inner diameter. The results in Fig. 6 show that the centrifugal effect also causes non-uniformity in the elastic deformation of the tooth surface. The maximum deformation occurs at the inner diameter and increases with the increasing centrifugal force. The relatively large elastic deformation region on the tooth surface gradually shrinks and increases the non-uniformity of the deformation on the tooth surface.

Figs.7 and 8 show the distributions of the slide distance and wear depth, respectively, on the tooth surface in a half cycle (0-max) when the speed is

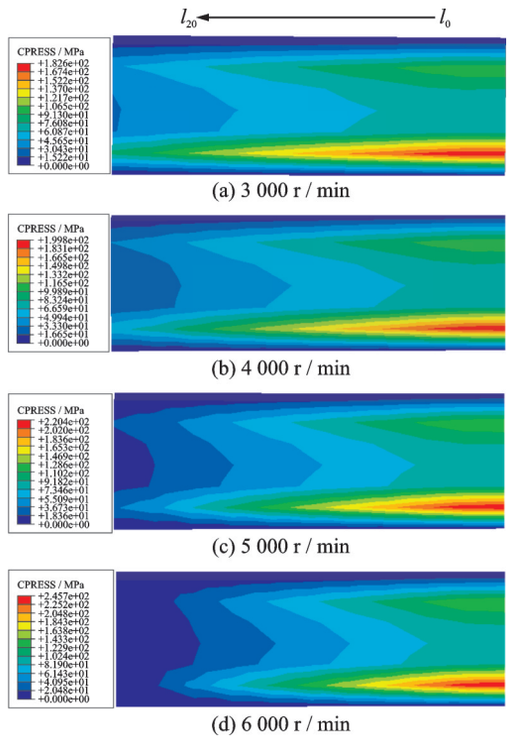

Fig.5 Contact stress at different rotational speeds

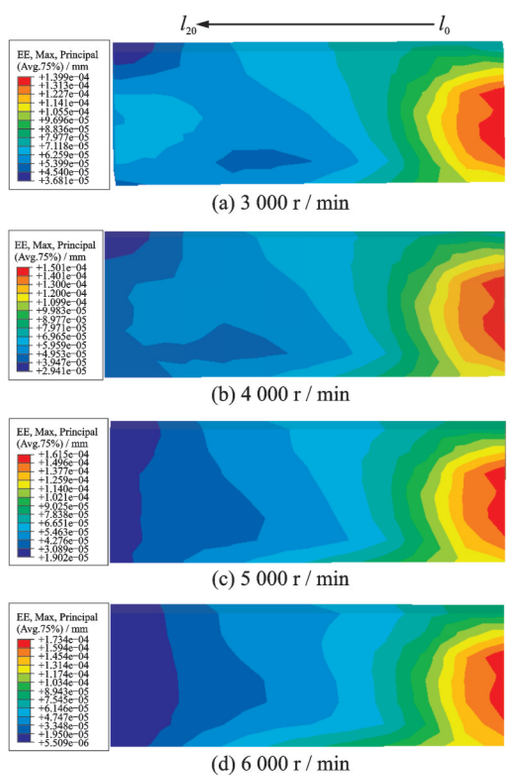

Fig.6 Elastic deformation at different rotational speeds

4 000 r/min. Fig.7 shows that the slide distance is the largest at the inner diameter side, and the slide distance gradually decreases from the inner diameter side to the outer diameter side, but there is no significant change in the tooth height direction. It can be

seen from Fig. 8 that the wear degree of the tooth surface gradually decreases from the inner diameter side to the outer diameter side of the tooth surface, with the degree of wear being the smallest on the outer side. In the tooth height direction, the wear at root position a_1 and the wear at tip position a_3 are both greater than that at the middle position of the tooth. The most severe wear of the tooth surface is on the inner diameter side of root position a_1.

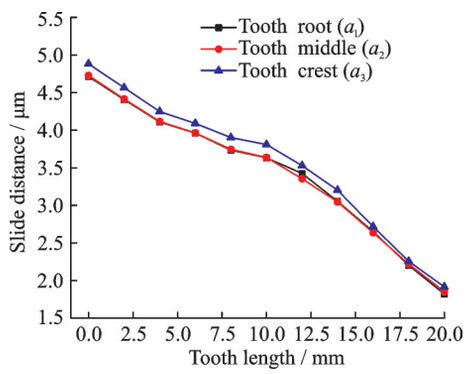

Fig.7 Slide distance distribution on internal tooth surface over half a cycle at a rotational speed of 4 000 r/min

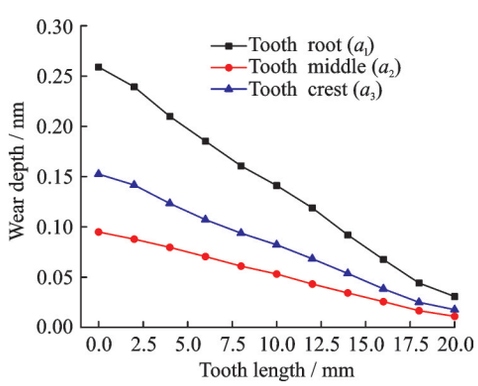

Fig.8 Wear depth distribution on internal tooth surface over half a cycle at a rotational speed of 4 000 r/min

Fig. 9 shows that, as the speed of rotation increased from 3 000 r/min to 6 000 r/min, the maximum tooth surface contact pressure increases from 182.04 MPa to 244.75 MPa, and the maximum slide distance increases from 4.169 μm to 5.323 μm. This is because the centrifugal effect tilts the contact tooth surface toward the inner diameter root position a_1 and results in excessive local stress that exceeds the local stresses in other locations. At the same time, when the speed increases from 3 000 r/min to

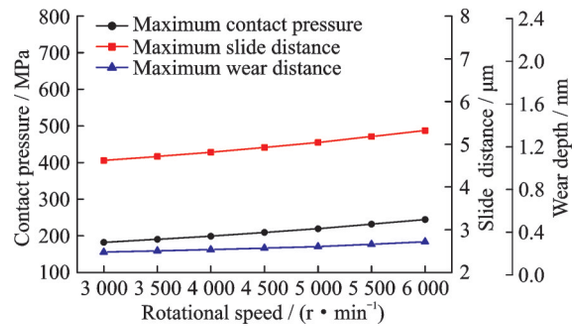

Fig.9 Maximum wear characteristics of tooth surface over half a cycle at different rotational speeds

6 000 r/min, the maximum wear depth of the tooth surface also increases from 0.214 nm to 0.311 nm.

2.2 Effects of temperature on fretting characteristics of face gear connection

Tie rod pre-tensioned combined rotors of aircraft engines often operate in high temperature and high pressure environments. The contact interface between assembled discs under ambient conditions will experience pronounced temperature gradients in the axial and radial directions at operating temperatures. In this study, the mutual constraint of the components in the rotor prevents the structure from free expansion or contraction and leads to considerable thermal stress on the contact surface. This in turn affects the degree of wear of the contact interface. For a torque of $T = 2\ 400$ N·m and a preload of 7.5 kN, the distributions of the contact stress and the elastic deformation on the tooth surface at different temperatures are shown in Figs. 10 and 11, respectively. Fig.10 shows that thermal expansion causes the two contacting surfaces to severely press against each other and produce a strong stress concentration. The contact stress is a maximum at the root position a_1, and the stress decreases along the height direction of the teeth. In addition, the contact stress increases significantly with the rising temperature. Fig. 11 shows that the temperature also has a great effect on the contact state of the tooth surface. The thermal expansion causes the major non-uniform deformation of the tooth surface. The maximum elastic deformation occurs at the median position a_2, causing the tooth surface to bulge slowly. The higher the temperature is, the greater the elas-

tic deformation of the contact surface is, and the greater the degree of unevenness is. The bulged shape becomes increasingly pronounced and concentrated toward the median position.

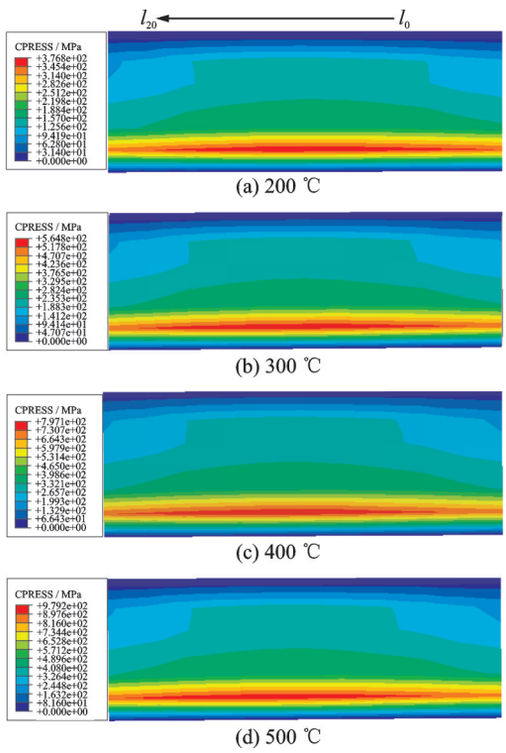

Fig.10 Contact stress at different temperatures

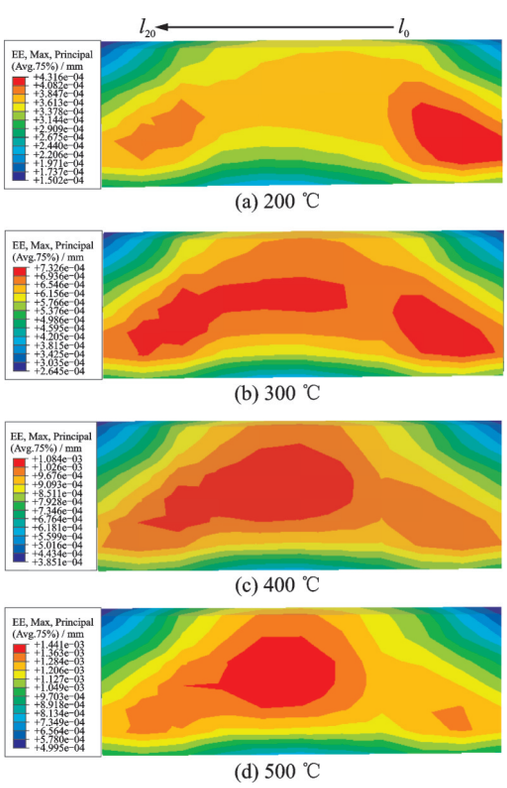

Fig.11 Elastic deformation at different temperatures

The results in Figs.12 and 13 show that under the action of the temperature, the distribution of the relative slide distance and the depth of wear become uneven, and the maximum slide distance and the maximum depth of wear both occur in the middle of the tooth root and continue to decrease along the tooth height direction. The contact stress, slide distance and wear depth at the tip portions a_3 are much less than those at the median position a_2 and the root portion a_1. The region with the most severe wear occurs at the root of the tooth.

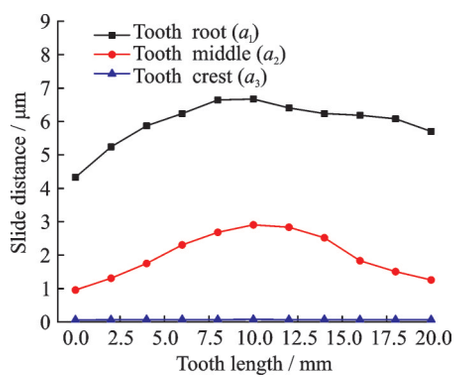

Fig.12 Slide distance distribution on tooth surface over half a cycle at 400 ℃

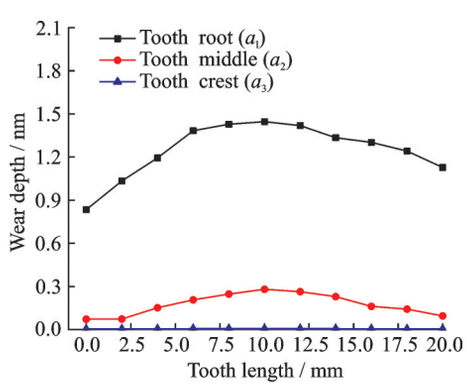

Fig.13 Wear depth distribution on tooth surface over half a cycle at 400 ℃

Fig.14 shows that the contact stress, slide distance and wear depth continue to increase significantly as the temperature rises. In the high temperature environment of 500 ℃, the maximum contact pressure can reach 979.2 MPa. The yield limit of the material has been exceeded at this time, but this is beyond the linear elasticity scope of this study. When the temperature increases from 200 ℃ to 500 ℃, the maximum wear depth of the tooth sur-

face increases sharply from 0.39 nm to 2.21 nm. This shows that the temperature has a great effect on the wear state of the tooth contact surface.

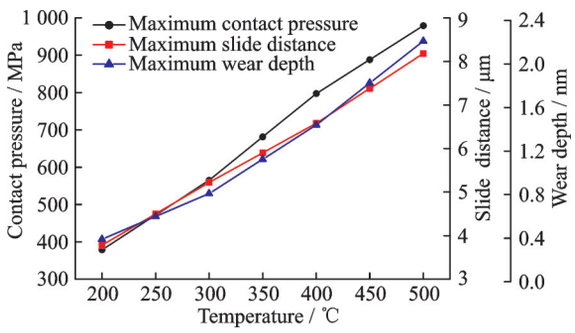

Fig.14 Maximum wear characteristics on tooth surface over half a cycle at different temperatures

2.3 Effects of coupled conditions on fretting characteristics of face gear connection

Fig.15 shows the effects of the temperature and the pre-tension coupling on the fretting characteristics of the tooth surface in contact during a half cycle at a torque of $T = 2\ 400$ N·m. This shows that due to the thermal expansion at high temperature, the contact surfaces become more fully intact and the relative slide distance tends to decrease. Therefore, the changes of the pre-tension at high temperature have a relatively small effect on the contact stress at the tooth surfaces. When the pre-tension increases from 9 kN to 23 kN, the maximum contact stress at the tooth surface remains essentially unchanged. The maximum slide distance increases from 7.51 μm to 8.62 μm, whose amplification is smaller than that at ambient temperature. And the maximum wear depth increases from 1.76 nm to 2.02 nm, whose amplification is essentially the same without considering the temperature effect.

Fig. 16 shows the coupling effects of the temperature and centrifugal force on the fretting characteristics of the tooth surface during half a cycle at a torque of $T = 2\ 400$ N·m and a preload of 7.5 kN. Fig.16(a) shows a slight decrease of the maximum contact stress at the tooth surface. This is caused by the weakening effect of the centrifugal tensile stress

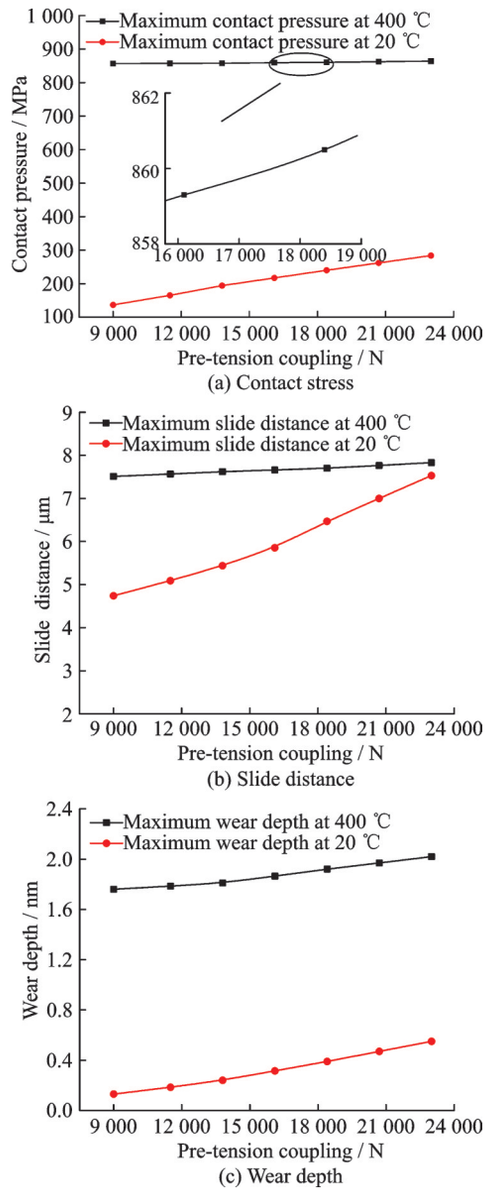

Fig.15 Effect of temperature and pre-tension coupling on fretting characteristics of tooth surface over half a cycle

on the stress concentration caused by the thermal expansion at high temperatures. When the rotational speed increases from 3 000 r/min to 6 000 r/min, the maximum contact stress on the tooth surface decreases from 848.5 MPa to 836.9 MPa. The maximum slide distance and the maximum wear depth of the tooth surface both increase with the increase of the centrifugal force, and the amplification is essentially the same as that without considering the temperature effect.

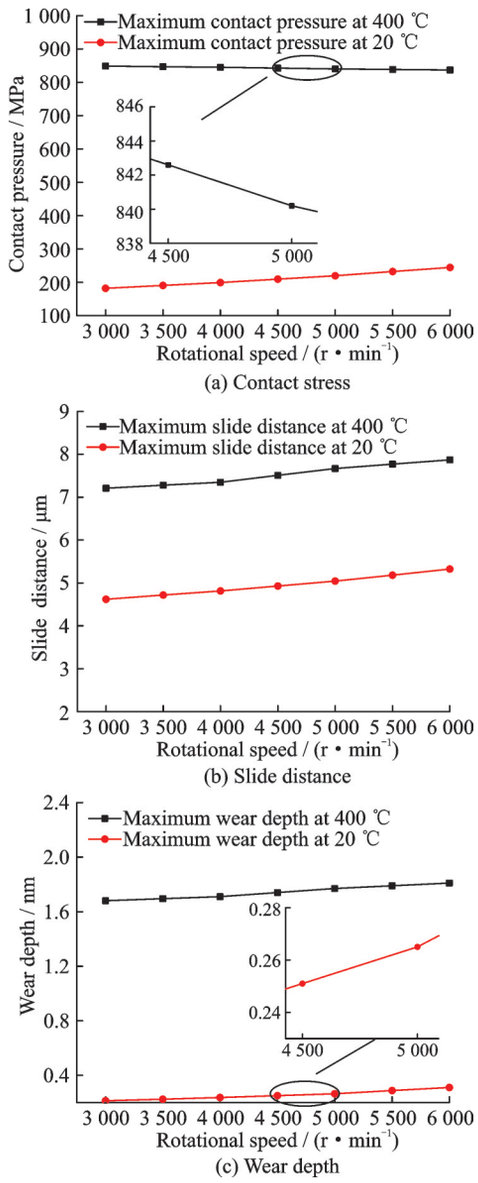

Fig.16 Effect of temperature and centrifugal force coupling on fretting characteristics of tooth surface over half a cycle

3 Conclusions

In order to examine typical connection structures of face gear in combined rotors, we analyze the variation behavior of the contact conditions, contact stress, slide distance, and wear depth of contacting tooth surfaces under different operating conditions. The following conclusions are drawn:

(1) The tensile stress produced by the centrifugal effect causes the contact surfaces of the face gear to separate and open at the outer diameter. This leads to a reduction of the load-bearing area, and the opening is greater at a higher rotational speed. The contact stress and the degree of wear are the greatest at the root on the inner diameter, and the wear increases with the increasing centrifugal force.

(2) Under the action of the temperature field, the contact surfaces expand due to heat and cause large non-uniform deformation. The center of the tooth surface forms a drum-shaped bulge. As the temperature rises, the contact stress and the wear depth of the tooth surface both increase sharply. At 400 ℃, the depth of the fretting wear increases to eight times that at ambient temperature. For this reason, it should be note to cool the rotor discs in actual operations.

References

[1] YUAN Qi, GAO Jin, LI Pu, et al. A review for structure and dynamic characteristics of heavy-duty gas turbine rotor[J]. Thermal Turbine, 2013, 42(4): 294-301.(in Chinese)

[2] MACBRIEN W. CT7-9 turboprop training guide [M]. Lynn, MA: GE Aircraft Engines, 1992.

[3] TAO Feng, ZHANG Xianfeng, YIN Mingde, et al. Research review on fretting damage: An review [J]. Journal of Nanjing University of Aeronautics & Astronautics, 1999, 31(5): 545-551. (in Chinese)

[4] HE Mingjian. Fretting fatigue of mechanical component [M]. Beijing: National Defense Industry Press, 1994. (in Chinese)

[5] PISANI S R, RENCIS J J. Investigating CURVIC coupling behavior by utilizing two- and three-dimensional boundary and finite element methods[J]. Engineering Analysis with Boundary Elements, 2000, 24(3): 271-275.

[6] RICHARDSON I J, HYDE T H, BECKER A A, et al. A validation of the three-dimensional finite element contact method for use with curvic couplings[J]. Proceedings of the Institution of Mechanical Engineers, Part G: Journal of Aerospace Engineering, 2002, 216(2): 63-75.

[7] YUAN S X, ZHANG Y Y, ZHANG Y C, et al. Stress distribution and contact status analysis of a bolted rotor with curvic couplings[J]. Proceedings of the Institution of Mechanical Engineers, Part C: Journal of Mechanical Engineering Science, 2010, 224(9): 1815-1829.

[8] YUAN Shuxia, ZHANG Youyun, JIANG Xiangjun, et al. Analysis of bolt preload mistuned model and its impact on stress distribution of curvic couplings[J]. Journal of Harbin Institute of Technology, 2013, 45

(5): 64-69.(in Chinese)

[9] LI Pu, YUAN Qi, GAO Jin, et al. Contact stress analysis of curvic coupling of circumferential tie rotor[J]. Thermal Turbine, 2013, 42(1): 25-29.(in Chinese)

[10] LU Mingjian. Research on structural strength design of heavy duty gas turbine combined rotor[D]. Xi'an: Xi'an Jiaotong University, 2017.(in Chinese)

[11] SHEN Xiang, CAO Peng. Contact state analysis of turboshaft engine rotor with curvic-coupling joint structure[J]. Aeroengine, 2017, 43(4): 35-40.(in Chinese)

[12] CHOI J W, KIM C S. A study on the stability of curvic coupling for distance to disk in a mill turret[J]. Applied Mechanics and Materials, 2011, 110/111/112/113/114/115/116: 1498-1505.

[13] LI Aimin. Research on design method of curvic couplings and fretting fatigue life prediction model[D]. Nanjing: Nanjing University of Aeronautics and Astronautics, 2015.(in Chinese)

[14] JIANG Xiangjun, ZHANG Youyun, YUAN Shuxia. An investigation and simulation of fretting wear of curvic in a gas turbine engine[J]. Journal of Harbin Institute of Technology, 2011, 43(3): 75-79.(in Chinese)

[15] LEEN S B, HYDE T R, WILLIAMS E J, et al. Development of a representative test specimen for frictional contact in spline joint couplings[J]. The Journal of Strain Analysis for Engineering Design, 2000, 35(6): 521-544.

[16] QI Wei. ABAQUS6.14 super learning manual[M]. Beijing: Posts & Telecom Press, 2016.(in Chinese)

[17] ZHUO Ming, YANG Lihua, XIA Kai. Contact stress analysis of combined rotor in heavy-duty gas turbine considering thermal effect[J]. Journal of Xi'an Jiaotong University, 2018, 52(11): 58-64.(in Chinese)

[18] DONG Dagin, YUAN Fengyin. Practical manual of pressure vessels and chemical equipment[M]. Beijing: Chemical Industry Press, 2008.(in Chinese)

[19] MCCOLL I R, DING J, LEEN S B. Finite element simulation and experimental validation of fretting wear[J]. Wear, 2004, 256(11/12): 1114-1127.

[20] SMITH K N, WATSON P, TOPPER T H. A stree-strain function for the fatigue of metals[J]. Journal of Materials, 1970, 5(4): 767-778.

Acknowledgements This work was supported by the National Natural Science of China (No.11872288) and the Natural Science Basic Research Plan in Shaanxi Province of China (No.2019JM-219).

Author Ms. **AN Xiuli** received her M.S. degree in Engineering Mechanics from Xi'an Jiaotong University, Shaanxi, China, in 2010. She is currently working in Xi'an Shaangu Power Co., Ltd and engaging in compressor technical support work. Her current research interest includes compressor structure design and strength calculation.

Author contributions Mrs. **An Xiuli** designed the study, conducted the analysis, interpreted the results, and wrote the manuscript. Mr. **PEI Dahai** contributed to the discussion and background of the study. Mr. **XIE Kun** contributed to data for the analysis. All authors commented on the manuscript draft and approved the submission.

Competing interests The authors declare no competing interests.

(Production Editor: ZHANG Huangqun)

端面齿接触界面温度/离心载荷微动磨损影响

安秀丽[1]，裴大海[1]，谢　坤[2]

(1.西安陕鼓动力股份有限公司，西安710075，中国；2.西安交通大学航天航空学院，西安710049，中国)

摘要：为了提高端面齿连接结构的可靠性，以组合转子的端面齿连接结构为研究对象，采用有限元方法研究了不同离心力和温度工况下接触齿面的接触状态、接触压力和滑移距离的分布规律，并基于McColl微动磨损模型研究了离心力和温度对齿面最大磨损深度的影响。结果表明：离心效应下，端面齿接触面会呈现外径分离张开的趋势，使承载面积减小，且端面齿内径侧齿根处的接触压力最大，磨损最严重；温度使接触面受热膨胀引起较大的不均匀变形，齿面呈现出鼓状，最大接触压力和最大磨损深度都发生在齿根的中部，且随温度升高，齿面最大接触压力和最大磨损深度会有较大幅度增大。因此，降低轮盘温度对减轻齿面磨损、提高连接寿命有重要作用。

关键词：端面齿；微动磨损；接触压力；磨损深度；微动磨损模型